DIMENSIONAL INFLUENCES ON THE RESPONSE OF A PV TRACKING SYSTEM

M.M. VĂTĂŞESCU[1]   **I. VIŞA**[1]   **D.V. DIACONESCU**[1]

Abstract: *Designing a bi-axial tracking linkage PV system rely on identifying the optimum dimensions to accomplish Sun's elevation and daily movements. To this effect the dimensional variations are needed to be ranked according to their influence on the tracking response. Thereby the optimum adjusting possibility and the allowable tolerance for each dimension are set. To obtain these results the partial derivate method is approached. In practice, the element having the first dimensional influence on tracking response is either provided with an adjustable system or is either imposed the highest dimensional precision. Herein, based on qualitative considerations, the second influencing length element is chosen to be the adjusted.*

Key words: *azimuth PV tracking system, dimensional influence, solar radiation, partial derivate method, tracking response.*

1. Introduction

According to the binding targets set up for wide Europe until 2020 [6], the renewable energy installed capacity projections for photovoltaic (PV) have to reach an annual growth rate of 23.6 between 2010 and 2020. In this scenario, Romania has to accomplish 24% share of energy form renewable sources in final consumption compared to the actual 18.2% [6].

Considering these objectives, one research direction in *Transilvania* University, Braşov is the improvement of PV solar tracking systems. Herein, one proposed solution is the bi-axial azimuth, mono-actuated, quadrilateral, spatial tracking system (Figure 1) designed to accomplish optimum tracking response: PV angular strokes very close to sun's elevation and azimuth for the Spring Equinox and tracking efficiency higher than 96% [1].

Two constructive variants were proposed for this model: a non-adjustable one (Figure 1a) and an adjustable one (Figure 1b), in which the screw device adjustment is set on the vertical pole (AB).

The proposed mechanism is a quadrilateral RRHH (*R* = rotating joint; *H* = Hook joint) spatial linkage which develops the out-put PV elevation displacement (α^*) from the input azimuth displacement (ψ^*), based on the action of a single actuator, according to the motion transmitting law (1) [1].

To simplify the letterings and calculus, (Figure 1), were considered the notations: *h* for vertical pole length, *l* for swing arm length, *r* for spatial radial linkage dimension and *e* for the distance between the vertical pole and the inferior Hook joint.

[1] Centre "Product Design for Sustainable Development", *Transilvania* University of Braşov.
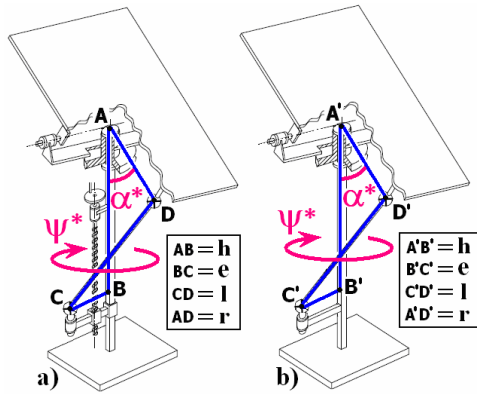
Fig. 1. *Two constructive variants for the azimuth tracking system: a) the adjustable and b) the non-adjustable* [1]

The explicit displacement function for the considered linkage is [1], [2], [4]:

$$\alpha^* = 2 \tan^{-1} \left(\frac{a \pm \sqrt{a^2 + b^2 - c^2}}{b + c} \right). \qquad (1)$$

In which:

$$a = 2 \cdot \frac{r \cdot \cos \psi^*}{e}, \qquad (1')$$

$$b = \frac{2hr}{e^2}, \qquad (1'')$$

$$c = \frac{r^2 + h^2 + e^2 - l^2}{e^2}. \qquad (1''')$$

To increase the tracking response of the given tracking linkage (Figure 1), three dimensional variants had been proposed [1], [2], [4], each computed after optimized algorithms and according to specific constraints.

Objectives: Considering the optimum dimensional solution reported in [1], present paper aims to rank each length dimensional influence on the response of the given tracking linkage (Figure 1) and so to assess the tolerance domain for each considered length: *h, r, l, e.* Moreover it will be demonstrated that *h* is the appropriate dimension to be adjusted on the given quadrilateral spatial tracking linkage (Figure 1). To that effect the partial derivate method is applied [3].

2. Analytical Modelling

To accomplish the upward stated objective and to simplify the calculus, the implicit motion transmitting law F (2) is developed around a considered point M_0 by calculating its partial derivate.

$F(\alpha^*, \psi^*, h, r, l, e) = 0$ is described in a 6-dimensioned space, impossible to render in our finite 3D reality. Therefore in Figure 2 is plotted an example of how is developed a function in 3D infinite small proximity of a chosen point M_0 (Figure 2a) and then transposed in 2D finite small proximity of the same point (Figure 2b).

In M_0 to F are assigned the values for *h, r, l, e,* ψ^* reported in [1], representing the optimum nominal tracking parameters for the considered linkage; corresponding α^* is computed according to (1).
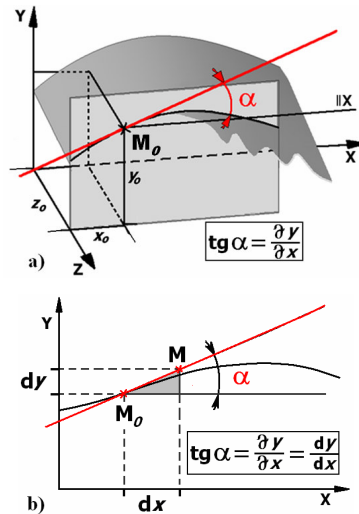

Fig. 2. *Function development in one M_0 point proximity: a) 3D and b) 2D case*

2.1. Modelling the Dimensional Variation Influences

To evaluate the effect of the dimensional infinite small variations Δh, Δr, Δl and Δe on the elevation displacement α^*, relation (1) must be derivate. Because implicit displacement law (1) is more complicated to derivate, the explicit form (2) is considered.

To rank the dimensional influences on α^*, partial derivates (3) are assumed for calculus [3]. Accordingly, each partial derivate (4), (5), (6), (7) and the corresponding finite small dimensional influence on α^* (4''), (5''), (6''), (7'') (Figure 2b) are computed:

$$F(\alpha^*,\psi^*,h,r,l,e) = 2r(e \cdot \sin\alpha^* \cdot \cos\psi^* + h \cdot \cos\alpha^*) + l^2 - r^2 - e^2 - h^2 = 0, \tag{2}$$

$$\frac{\partial F}{\partial x}\mathrm{d}x = 0 \;\Rightarrow\; \frac{\partial\alpha^*}{\partial x}, \; x = \{h, \, r, \, l, \, e\}, \tag{3}$$

$$\boldsymbol{x = h} \Rightarrow \frac{\partial F}{\partial h} = 2re \cdot \cos\psi^* \cdot \frac{\partial\alpha^*}{\partial h} \cdot \cos\alpha^* + \left[2r \cdot \cos\alpha^* - 2rh \cdot \frac{\partial\alpha^*}{\partial h} \cdot \sin\alpha^*\right] - 2h = 0, \tag{4}$$

$$\frac{\partial\alpha^*}{\partial h} = \frac{h - r \cdot \cos\alpha^*}{r(e \cdot \cos\psi^* \cos\alpha^* - h \cdot \sin\alpha^*)} \;\Rightarrow\; \Delta\alpha^* = \frac{\partial\alpha^*}{\partial h} \cdot \Delta h, \tag{4'; 4''}$$

$$\boldsymbol{x = r} \Rightarrow \frac{\partial F}{\partial r} = \left[2e \cdot \cos\psi^* \sin\alpha^* + 2re \cdot \cos\psi^* \cdot \frac{\partial\alpha^*}{\partial r} \cdot \cos\alpha^*\right] + ...$$
$$... + \left[2h \cdot \cos\alpha^* - 2rh \cdot \frac{\partial\alpha^*}{\partial r} \cdot \sin\alpha^*\right] - 2r = 0, \tag{5}$$

$$\frac{\partial\alpha^*}{\partial r} = \frac{r - h \cdot \cos\alpha^* - e \cdot \cos\psi^* \sin\alpha^*}{r(e \cdot \cos\psi^* \cos\alpha^* - h \cdot \sin\alpha^*)} \Rightarrow \Delta\alpha^* = \frac{\partial\alpha^*}{\partial r} \cdot \Delta r, \tag{5'; 5''}$$

$$\boldsymbol{x = l} \Rightarrow \frac{\partial F^*}{\partial l} = 2re \cdot \cos\psi^* \cdot \frac{\partial\alpha^*}{\partial l} \cdot \cos\alpha^* - 2rh \cdot \frac{\partial\alpha^*}{\partial l} \cdot \sin\alpha^* + 2l = 0, \tag{6}$$

$$\frac{\partial\alpha^*}{\partial l} = \frac{-l}{r(e \cdot \cos\psi^* \cos\alpha^* - h \cdot \sin\alpha^*)} \Rightarrow \Delta\alpha^* = \frac{\partial\alpha^*}{\partial l} \cdot \Delta l, \tag{6'; 6''}$$

$$\boldsymbol{x = e} \Rightarrow \frac{\partial F}{\partial e} = \left[2r \cdot \cos\psi^* \cdot \sin\alpha^* + 2re \cdot \cos\psi^* \cdot \frac{\partial\alpha^*}{\partial e} \cdot \cos\alpha^*\right] - ...$$
$$... - 2rh \cdot \frac{\partial\alpha^*}{\partial e} \cdot \sin\alpha^* - 2e = 0, \tag{7}$$

$$\frac{\partial\alpha^*}{\partial e} = \frac{e - r \cdot \cos\psi^* \sin\alpha^*}{r(e \cdot \cos\psi^* \cos\alpha^* - h \cdot \sin\alpha^*)} \Rightarrow \Delta\alpha^* = \frac{\partial\alpha^*}{\partial e} \cdot \Delta e. \tag{7'; 7''}$$

2.2. Numerical Simulations

To evaluate the effects that each dimension variation has on the tracking response, the last dimensional results [1] are considered. Therein the number of four unknown length dimensions (h, r, l, e) were reduced to three unknown dimensionless ratios: $H = h/e$; $R = r/e$; $L = l/e$, in which $e = 1$. Herein, $e = 0.3$ m is considered; therefore the values in Table 1 are obtained, representing h, r, l, e values in M_0 where F is analyzed.

Table 1

Seasonal reduced dimensions for the adjustable [1] and the non-adjustable tracking linkages

	h	r	l	e
	[m]			
Adjustable tracking linkage				
Spring/Autumn	0.873	0.582	0.474	0.3
Summer	0.699	0.582	0.474	0.3
Winter	0.909	0.582	0.474	0.3
Non-adjustable tracking linkage				
All seasons	0.873	0.582	0.474	0.3

To identify the optimum dimension to be adjusted (the length dimension with the highest influence on α^*) are considered the deviations: $\Delta h = \Delta r = \Delta l = \Delta e = 20$ mm (0.02 m). The results are used to also identify the appropriate manufacturing precision.

The proposed azimuth tracking system was dimensional configured to attain an optimum seasonal adaptability to sun's elevation movement [1], [2], [4]. To obtain relevant results through numerical simulations, the representative seasonal days in the year are considered: Spring Equinox (considered similar to the Autumn Equinox [1], [2], [5]), Summer Solstice and Winter Solstice.

First, the dimensional influences for both the adjustable and the non-adjustable tracking linkages are numerically simulated, according to relations (3'), (4'), (5') and (6'), during the above mentioned representative seasonal days (Figures 3 and 4). In all cases, the curves indicate that l dimensional variation has the highest influence on PV's elevation stroke and e dimensional variation has the lowest influence. Accordingly, h is the second parameter with high influence on α^*.

To assess the measurable effects of these dimensional influences, in Figures 5 and 6 are plotted PV's elevation daily variations corresponding to each modified dimension $(h + \Delta h)$; $(r + \Delta h)$; $(l + \Delta l)$; $(e + \Delta e)$. The hierarchy of dimensional influences on α^* is the same as before: l - the first, h - the second, r - the third and e - the last length element affecting α^* precision.

Deflections of α^* in Figures 5 and 6 affect sunray's incidence angle on the PV surface (Figure 7) [5]: in spring, autumn and winter the incidence values corresponding to h, l, r, e variations are parted from the initial optimum ones (Figure 7a, c). Because, the incidence angle influences directly the solar radiation gain [1], [2], [5], then h, l, r, e dimensional variations come to affect as well the corresponding solar radiation yield, by diminishing it during the up-mentioned seasons (Figure 8a, c).

Though, an opposite situation can be noticed in Figure 7b where by extending h with the considered $\Delta h = 20$ mm an improved incidence angle is obtained and a higher solar radiation is harvest (Figure 8b) in the summer season.

3. Results and Discussion

The situation presented in Figures 3-6 is confirmed by the seasonal maximum PV's elevation deviations in Table 2. Accordingly is being identified that l is the length element with the highest dimensional variation influence on PV's elevation angular stroke, for both the adjustable and the nonadjustable tracking linkages. This means that l should theoretically be the adjustable element, when considering the

adjustable model, or the element with the highest dimensional precision in manufacturing, when considering the non-adjustable model. Though, the adjusting screw system can not be attached to *l*-swing arm due to its restricted mechanical resistance (e.g. on windy conditions). Therefore it is appropriate to adjust *h*-length (the second most influencing dimensional element on PV's elevation angular stroke) when designing the adjustable linkage.
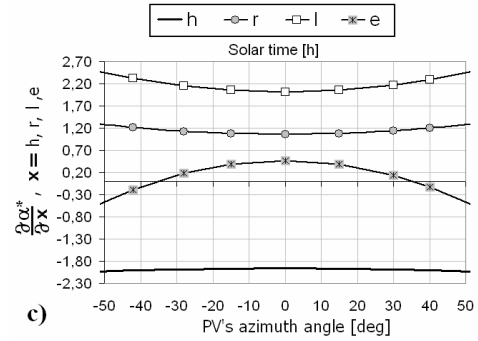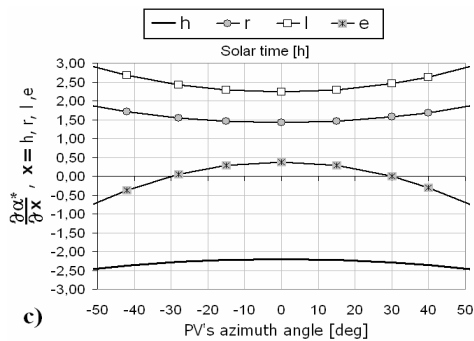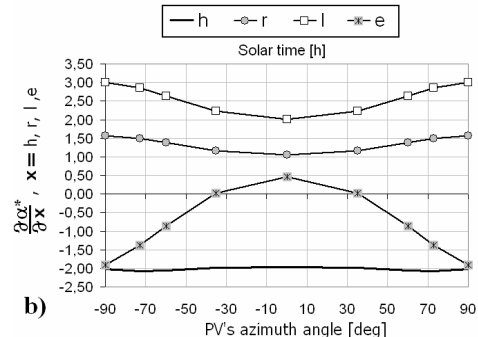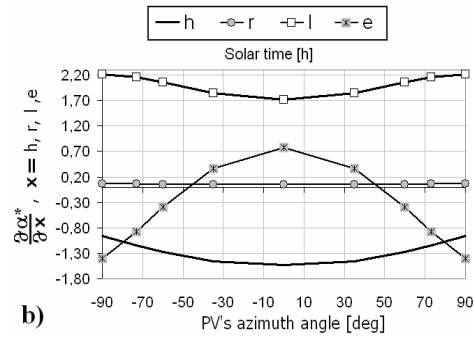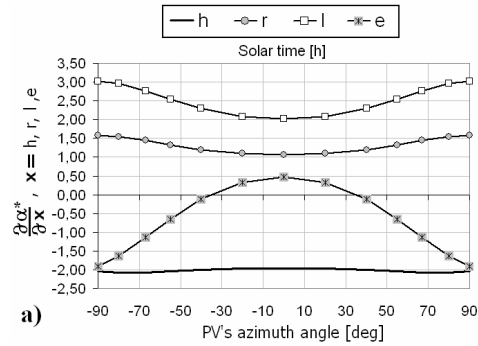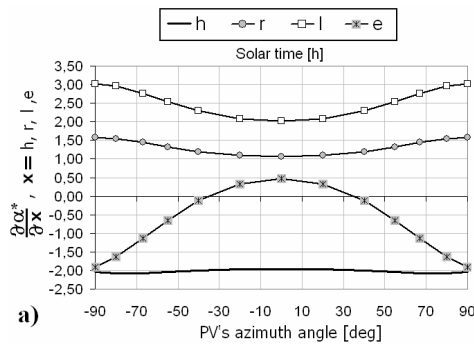
Fig. 3. *PV's elevation partial derivate variations for the adjustable linkage PV's elevation angle* (α^*) *during a) Spring Equinox; b) Summer Solstice and c) Winter Solstice*

Fig. 4. *PV's elevation partial derivate variations on the non-adjustable linkage PV's elevation angle* (α^*) *during a) Spring Equinox; b) Summer Solstice and c) Winter Solstice*
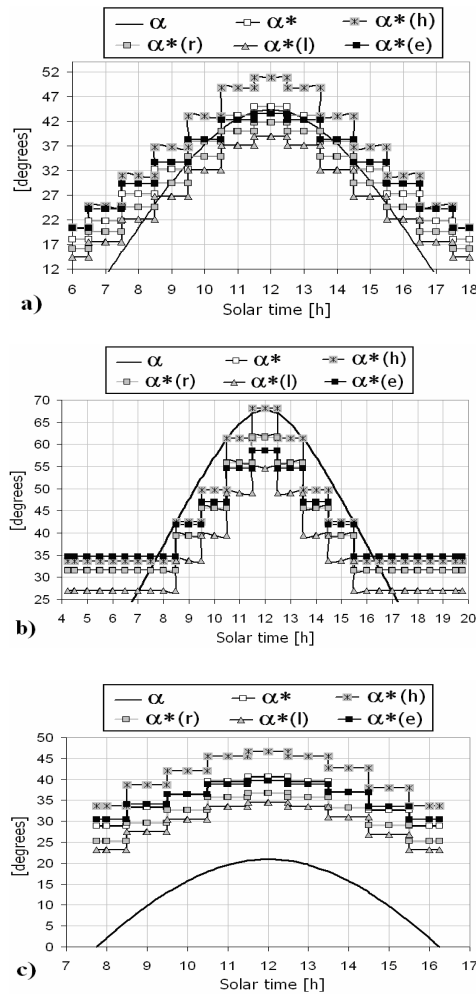
Fig. 5. $\Delta h = \Delta r = \Delta l = \Delta e = 20$ mm
Influences on the adjustable linkage PV's elevation angle (α^*) during a) Spring Equinox; b) Summer Solstice and c) Winter Solstice

Fig. 6. $\Delta h = \Delta r = \Delta l = \Delta e = 20$ mm
Influences on the non-adjustable linkage PV's elevation angle (α^*) during a) Spring Equinox; b) Summer Solstice and c) Winter Solstice

The aspects presented in Table 2 are sustained by the values in Table 3: higher the deflection is on the elevation angle, larger is the incidence angle deviation.

The influence is inverted between the incidence angle and the received solar radiation (Table 4). Therefore: higher the incidence angle deviation, the more diminished the gain solar radiation.

4. Conclusions

In this paper is identified the optimum dimensional adjustment possibility for the azimuth mono-actuated tracking linkage. Accordingly, the hierarchy of dimensional variation influences on tracking response is set through partial derivate calculus, so the length elements are ranked: *l* - the first, *h* - the

second, *r* - the third and *e* - the last length element affecting the tracking response. Accordingly for the non-adjustable model *l*

is assessed having the highest dimensional precision whereas to *e* is assigned the lowest. For the adjustable model, theoretically
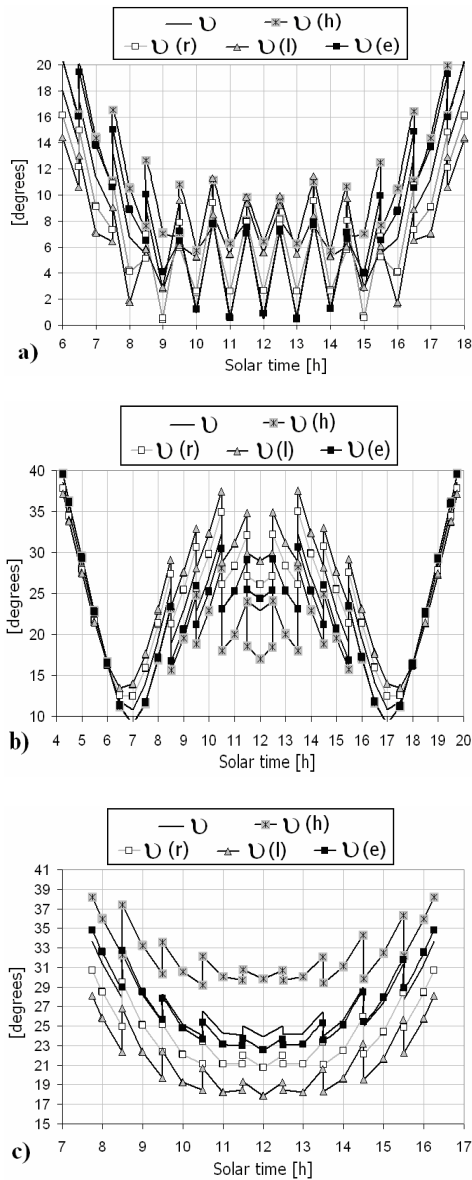

Fig. 7. $\Delta h = \Delta r = \Delta l = \Delta e = 20$ mm
Influences on the incidence angle for the non-adjustable linkage during: a) Spring Equinox; b) Summer Solstice and c) Winter Solstice
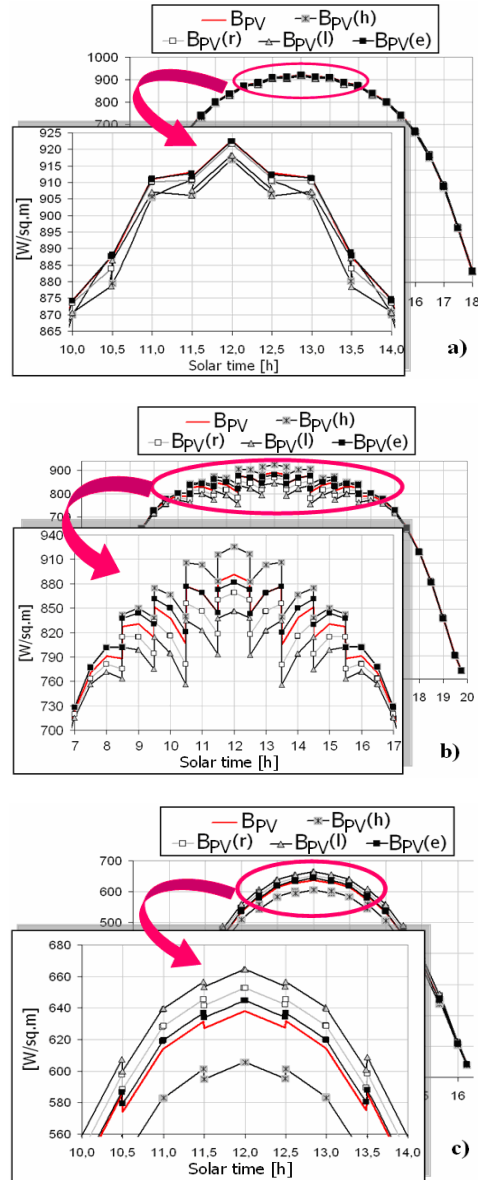
Fig. 8. $\Delta h = \Delta r = \Delta l = \Delta e = 20$ mm
Influences on the received direct solar radiation for the non-adjustable mechanism during: a) Spring Equinox; b) Summer Solstice and c) Winter Solstice

Table 2

Seasonal maximum PV elevation deviations from α^* in M_0 when enlarging with 20 mm each h, r, l, e (Figs. 5 and 6)

	$\Delta\alpha^*(h)$	$\Delta\alpha^*(r)$	$\Delta\alpha^*(l)$	$\Delta\alpha^*(e)$
Adjustable tracking linkage				
Spring/ Autumn	+5.9°	−3.2°	−6.1°	−1.4°
Summer	−6.4°	−0.2°	−7.1°	−3.2°
Winter	+6°	−3.9°	−6.1°	−1°
Non-adjustable tracking linkage				
All seasons	+5.9°	−3.2°	−6.1°	−1.4°

Table 3

Seasonal maximum incidence angle deviations from ν in M_0 when enlarging with 20 mm each h, r, l, e (Fig. 7)

	$\Delta\nu(h)$	$\Delta\nu(r)$	$\Delta\nu(l)$	$\Delta\nu(e)$
Adjustable tracking linkage				
Spring/ Autumn	+5.9°	+2.1°	+5°	+0.4°
Summer	−5.8°	+0.2°	+7.1°	+3,2
Winter	+6°	−3.9°	−6.1°	−1°
Non-adjustable tracking linkage				
All seasons	+5.9°	+2.1°	+5°	+0.4°

Table 4

Seasonal maximum direct solar radiation deflections from B_{PV} in M_0 when enlarging with 20 mm each h, r, l, e (Fig. 8)

	ΔB_{PV} (h)	ΔB_{PV} (r)	ΔB_{PV} (l)	ΔB_{PV} (e)
[W/m^2]				
Adjustable tracking linkage				
Spring/ Autumn	−9.1	+4.7	+7.8	−4.5
Summer	+5	−0.8	−30.9	−7.8
Winter	−28	+14.4	+21.2	+4
Non-adjustable tracking linkage				
All seasons	−9.1	+4.7	+7.8	−4.5

l should be the adjustable element; practically, it is a slender element and an adjustable *l* (e.g. a telescopic structure) would cause instability upon the entire system. Therefore the adjusting screw device is attached on the vertical pole *h* (the second most important length element on affecting the tracking response).

The results are used to also identify the appropriate manufacturing precision.

References

1. Diaconescu, D.V., et al.: *The Optimization of a Bi-Axial Adjustable Mono-actuator PV Tracking Spatial Linkage.* In: Proceedings of EUCOMES Conference, Springer, Cluj, Romania, 2010.
2. Diaconescu, D.V., et al.: *Synthesis of a Bi-Axial Tracking Spatial Linkage with a Single Actuator.* In: Proceedings of SYROM 2009, Springer, 2009, p. 632-617.
3. Dudiţă, F., et al.: *Transmisii cardanice* (*Cardanic Transmissions*). Braşov. Transilvania Express, 2003.
4. Vătăşescu, M., et al.: *On the Simulation of a Mono-Actuator Bi-Axial Azimuth PV System.* In: Bulletin of the *Transilvania* University of Braşov, Vol. 2 (51), Series I, 2009, p. 97-104.
5. Vişa, I., et al.: *On the Incidence Angle Optimization of the Dual-Axis Solar Tracker.* In: 11th International Research/ Expert Conference TMT-Trends in the Development of Machinery and Associated Technology, Hammamet, Tunisia, 2007, p. 1111-1114.
6. http://www.erec.org/fileadmin/erec_docs/ Documents/Publications/Renewable_ Energy_Technology_Roadmap.pdf. Accesed: 19-05-2010.